

K^+ -nucleus potentials from K^+ -nucleon amplitudes

E. Friedman^{a,*}

^a*Racah Institute of Physics, The Hebrew University, 91904 Jerusalem, Israel*

Abstract

Optical potentials for K^+ -nucleus interactions are constructed from K^+ -nucleon amplitudes using recently developed algorithm based on K^+ -N kinematics in the nuclear medium. With the deep penetration of K^+ mesons into the nucleus at momenta below 800 MeV/c it is possible to test this approach with greater sensitivity than hitherto done with K^- and pions. The energy-dependence of experimental reaction and total cross sections on nuclei is better reproduced with this approach compared to fixed-energy amplitudes. The inclusion of Pauli correlations in the medium also improves the agreement between calculation and experiment. The absolute scale of the cross sections is reproduced very well for ${}^6\text{Li}$ but for C, Si and Ca calculated cross sections are $(23\pm 4)\%$ smaller than experiment, in agreement with earlier analyses. Two phenomenological models that produce such missing strength suggest that the imaginary part of the potential needs about 40% enhancement.

Keywords: K^+ -nucleon amplitudes, K^+ -nucleus optical potentials, K^+ -nucleus reaction and total cross section, medium-dependent effects

1. Introduction and background

The connection between hadron-nucleus interaction and the corresponding hadron-nucleon interaction could provide information on possible modifications of strong interaction properties in the nuclear medium. The interaction of low energy pions with nuclei, and pionic atoms in particular, is a good example where the dominance of the P -wave (3,3) resonance in the pion-nucleon interaction underlies the Kisslinger [1] and the Ericson-Ericson [2]

*Corresponding author: E. Friedman, elifried@cc.huji.ac.il

models for the pion-nucleus interaction. The depth of penetration of a meson into the nucleus is a key element in this connection and indeed below 80 MeV empirical pion-nucleus potentials display the characteristics of the P -wave model [3]. As the pion energy increases towards the resonance with the associated increased absorption, it is found that good description of the pion-nucleus interaction is possible also without an explicit P -wave model [4, 5].

The present work deals with K^+ meson-nucleus interaction at low energies where the total K^+ -nucleon cross sections are small and the kaon penetrates well into the nucleus. This property of the K^+ is well known [6] and some experiments in the 1990s were motivated by it [7, 8, 9, 10]. The present study was inspired by recent works [11, 12, 13, 14, 15, 16, 17, 18, 19] where algorithms based on *in-medium kinematics* have been applied in calculations of optical potentials from the corresponding hadron-nucleon scattering amplitudes.

Applying this approach to K^+ mesons, the kaon-nucleon scattering amplitude is presented in terms of the Mandelstam variable s in the nuclear medium

$$s = (E_K + E_N)^2 - (\vec{p}_K + \vec{p}_N)^2, \quad (1)$$

where $E_K = m_K + E_{\text{lab}}$, $E_N = m_N - B_N$. E_{lab} is the laboratory kinetic energy of the kaon and B_N is an average binding energy of a nucleon. In the nuclear medium $\vec{p}_K + \vec{p}_N \neq 0$ where \vec{p}_K is determined by the beam energy and the optical potential, \vec{p}_N is determined by the nuclear environment. Averaging over angles, $(\vec{p}_K + \vec{p}_N)^2 \rightarrow (p_K)^2 + (p_N)^2$. Substituting locally

$$p_K^2/2m_K \rightarrow E_{\text{lab}} - \text{Re } V_{\text{opt}}^K - V_c, \quad (2)$$

with V_{opt}^K the kaon-nucleus optical potential and V_c the Coulomb potential. For the nucleon the Fermi gas model yields

$$p_N^2/2m_N \rightarrow T_N(\rho/\bar{\rho})^{2/3} \quad (3)$$

with $T_N=23$ MeV the average kinetic energy, ρ and $\bar{\rho}$ the local and average nuclear densities, respectively.

The simplest ' $t\rho$ ' form of the optical potential is [20]

$$2\epsilon_{\text{red}}^{(A)} V_{\text{opt}}^K(r) = -4\pi F_A b_0(\sqrt{s})\rho(r) \quad (4)$$

where $\epsilon_{\text{red}}^{(A)}$ is the c.m. reduced energy

$$(\epsilon_{\text{red}}^{(A)})^{-1} = E_p^{-1} + E_A^{-1} \quad (5)$$

in terms of the total energies E_p for the projectile and E_A for the target and

$$F_A = \frac{M_A \sqrt{s}}{m_N (E_A + E_p)} \quad (6)$$

is a kinematical factor resulting from the transformation of amplitudes between the projectile-nucleon and the projectile-nucleus systems. b_0 is the isospin-averaged free K^+ -N forward scattering amplitude.

Defining $\delta\sqrt{s} = \sqrt{s} - E_{\text{th}}$ with $E_{\text{th}} = m_K + m_N$, then to first order in B/E_{th} and $(p/E_{\text{th}})^2$ one gets [15]

$$\delta\sqrt{s} - \xi_N E_{\text{lab}} = -B_N \rho / \bar{\rho} - \xi_N T_N (\rho / \bar{\rho})^{2/3} + \xi_K [\text{Re } V_{\text{opt}} + V_c (\rho / \rho_0)^{1/3}], \quad (7)$$

with $\xi_N = m_N / (m_N + m_K)$, $\xi_K = m_K / (m_N + m_K)$. This value of \sqrt{s} serves as the argument of the *in medium* kaon-nucleon amplitude in constructing the kaon-nucleus optical potential.

Figure 1 shows the isospin-averaged K^+ -nucleon amplitude as function of the c.m. energy \sqrt{s} , taken from the SAID software package [21] including S, P and D partial waves. Vertical dashed lines indicate the energies corresponding to the four experimental energies considered in the present work. It is seen that the variation of the imaginary part of the amplitude is significant and could result in observable effects within the above algorithm.

With the relatively small K^+ -N total cross sections below 800 MeV/c kaons penetrate deeply into nuclei and the above algorithm can be tested with greater sensitivity than before. In analyses of pionic atoms since true absorption is impossible on a single nucleon, a two-nucleon phenomenological term is always present in the potential that fits experimental results. Similarly phenomenological two-nucleon terms are found in analyses of elastic scattering of π^\pm by nuclei at low energies. For K^- atoms multi-nucleon terms are found when comparing calculations with experiment. For η mesons there are no experimental results yet for η -nucleus interaction to compare with. For anti-protons there is a vast collection of experimental results but the very strong absorption precludes a real test of the above algorithm in the nuclear medium. Consequently the K^+ -nucleus below 800 MeV/c is a preferred probe because there are experimental results to compare with and

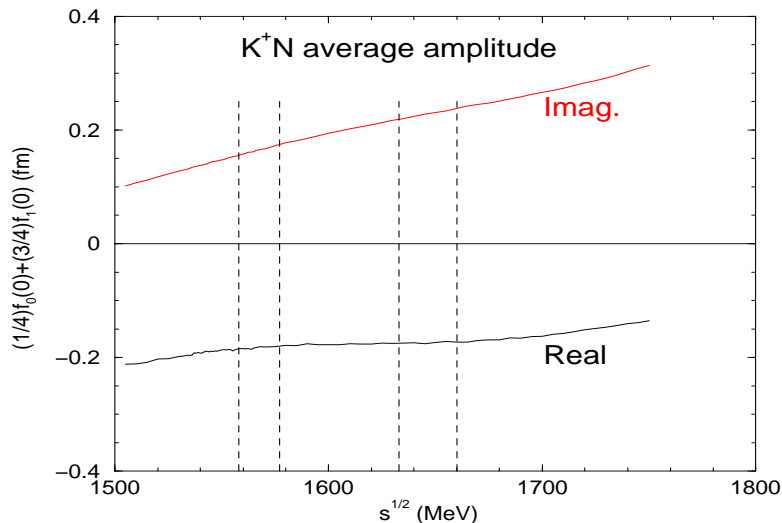


Figure 1: Isospin-averaged K^+ -nucleon amplitudes. Vertical dashed lines indicate the four experimental energies discussed in the present work.

there is no evidence that there are significant multi-nucleon contributions. In the present work we use mostly reaction and total cross sections on nuclei as these have been measured to good accuracy. Few experimental angular distributions for elastic scattering of K^+ by C are discussed below.

In section 2 we briefly review past work on the topic of K^+ -nucleus integral cross sections and in section 3 we apply the above approach to compare between experimental results and calculations. Section 4 is summary and conclusions.

2. K^+ -nucleus integral cross sections

The pioneering experiment of Bugg et al. [6] showed that above 800 MeV/c total cross sections for K^+ on carbon were smaller than six times the corresponding cross sections on deuteron, as expected. In contrast, below that momentum the reverse was true, exhibiting enhancement of the nuclear total cross section relative to the nucleon cross section. This statement obviously depends on the assumption that nuclear medium effects on the deuteron are very small. Later Siegel, Kaufmann and Gibbs [22] showed that calculations of the ratio K^+ -carbon to K^+ -deuteron total cross sections which included

traditional medium corrections and their uncertainties, failed to reproduce the above enhancement, thus suggesting more exotic mechanisms. Several publications that followed considered density-dependent effective masses of the vector mesons [23], meson exchange current [24], pion cloud contribution [25] and mesons exchanged between the K^+ and the target nucleons [26].

The experimental situation with K^+ -nucleus interactions changed when in the early 1990s total cross sections for D, ${}^6\text{Li}$, ${}^{12}\text{C}$, Si and Ca were measured at four momenta below 800 MeV/c [7, 8, 9, 10]. The method was to measure transmissions through a target using detectors subtending different solid angles and extrapolating to zero solid angle after applying model-dependent corrections. The same set of transmission measurements was later reanalysed [27] to determine not only total cross sections but also total reaction cross sections that are less dependent on applied corrections. That increased the number of measured integral cross sections from 16 to 32, in addition to those on D. Self-consistent analyses of this set of data [28, 29] confirmed that the cross sections on C, Si and Ca were 15-20% larger than expected compared to D and to the very low-density nucleus ${}^6\text{Li}$. Phenomenological fits to the data required mainly increased imaginary part of the effective K^+ -nucleon amplitudes in the medium. Analysis of the same data by Peterson [30] in terms of an average S -wave phase-shift showed good agreement with experiment when increasing this phase-shift in the medium relative to free space. A possible link between the additional reactive content and K^+ interactions with two nucleons was explored in [31, 32].

3. Results

Table 1: Comparisons between total cross sections (in mb) of K^+ on ${}^6\text{Li}$ with three times the cross sections on deuteron. Only statistical errors are quoted.

p_{lab} (MeV/c)	488	531	656	714
$3\times\text{D}$	76 ± 1.8	81.5 ± 1.0	84.5 ± 0.7	86.0 ± 0.6
${}^6\text{Li}$	77.5 ± 1.1	80.7 ± 0.7	86.4 ± 0.7	88.5 ± 0.6

The experimental results used in the present analysis are reaction and total cross sections for K^+ on ${}^6\text{Li}$, C, Si and Ca from Ref.[29]. Total cross sections on D are taken from Ref.[27]. Table 1 compares total cross sections

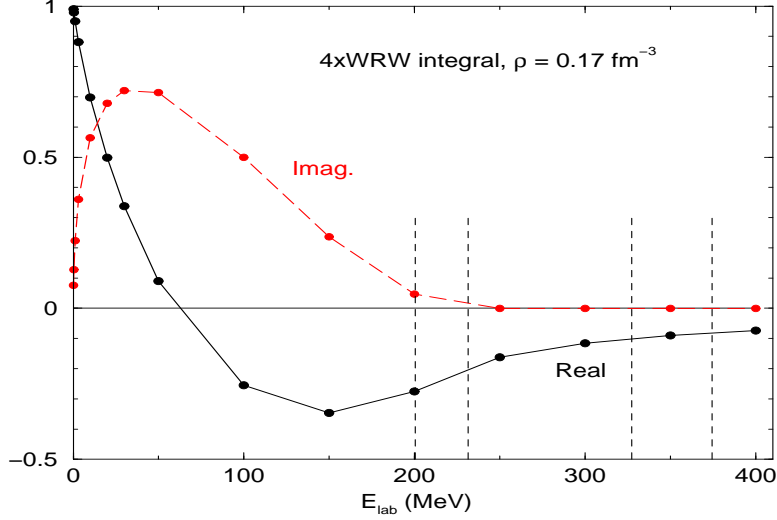


Figure 2: Four times the integral of Eq.(9) as function of energy for a full nuclear density. Vertical dashed lines indicate the experimental energies.

of K^+ on ${}^6\text{Li}$ with three times the cross sections on deuteron. It is seen that within 2% there are no indications for medium effects in the results for ${}^6\text{Li}$, where the average density is about half of the average density for other nuclei. Consequently in what follows we use ${}^6\text{Li}$ as a reference.

3.1. Testing in-medium kinematics

Before applying Eq.(7) to calculate K^+ -nucleus cross sections it is necessary to correct the free K^+ -nucleon amplitudes by considering Pauli correlations. The corrections of Waas, Rho and Weise (WRW) [33] replace $F_A b_{0\rho}$ of Eq.(4) by

$$\sum_I \frac{2I+1}{4} \frac{F_A f_I}{1 + \frac{1}{4}\xi F_A f_I \rho(r)} \rho(r) \quad (8)$$

where f_I are the isospin I free K^+ -nucleon forward scattering amplitudes. Therefore the medium corrections are determined by the quantity

$$\xi = \frac{9\pi}{p_F^2} \left(4 \int_0^\infty \frac{dt}{t} \exp(iqt) j_1^2(t) \right), \quad q = k/p_F. \quad (9)$$

where $k = (\omega_K^2 - m_K^2)^{1/2}$ with ω_K the c.m. energy and the Fermi momentum p_F given by $p_F = (3\pi^2\rho/2)^{1/3}$. For kaonic atoms $k \approx 0$ and the expression

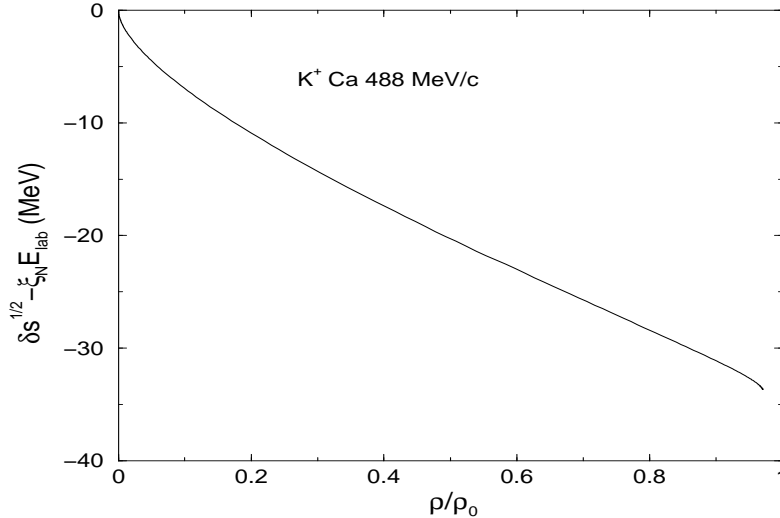


Figure 3: Example of density to energy transformation implied by Eqs.(4) and (7).

in brackets is 1, but for scattering ($k \neq 0$) the integral (and the corrections) go down rapidly with increasing energy. Figure 2 shows as an example, four times the above integral as function of energy for a Fermi momentum corresponding to central nuclear density.

Equations (4) and (7) define a density to energy transformation through the scattering amplitudes. As the real part of the potential determines the energy and, in turn, the energy and density determine the amplitudes, a self-consistent solution is required. Good convergence is usually achieved after 4-5 iterations and an example for this transformation is shown in Fig. 3 for 488 MeV/c K^+ interacting with Ca. An energy range of 30 MeV that corresponds to penetration of the kaon into regions of up to full nuclear density could be significant, as can be seen from Fig. 1

As a first step in comparisons between calculation and experiment we show in the top part of Fig. 4 reaction and total cross sections on ${}^6\text{Li}$. The calculations use amplitudes at *fixed* energies related to the beam energies without respecting Eq.(7) and without the Pauli correlation correction (WRW). Ratios of experimental to calculated cross sections are shown for the four energies, alternating between reaction (R) and total (T) cross sections. It is gratifying that to within 5% the calculations reproduce the absolute scale of the experimental results. However, upon closer examination it is clear that

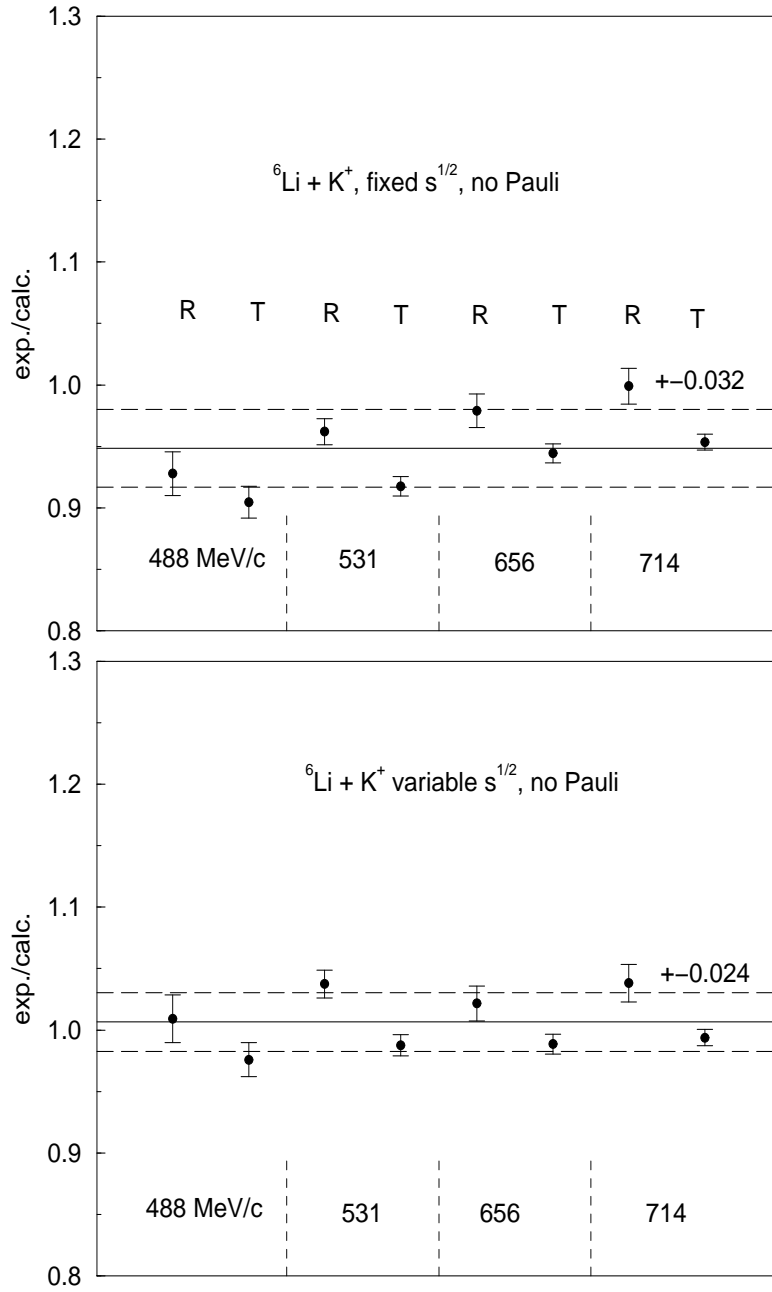


Figure 4: Experimental to calculated ratios of reaction and total cross sections on ${}^6\text{Li}$ for fixed energies (top) and for variable energies Eq.(7) (bottom). R and T indicate reaction and total cross sections, respectively.

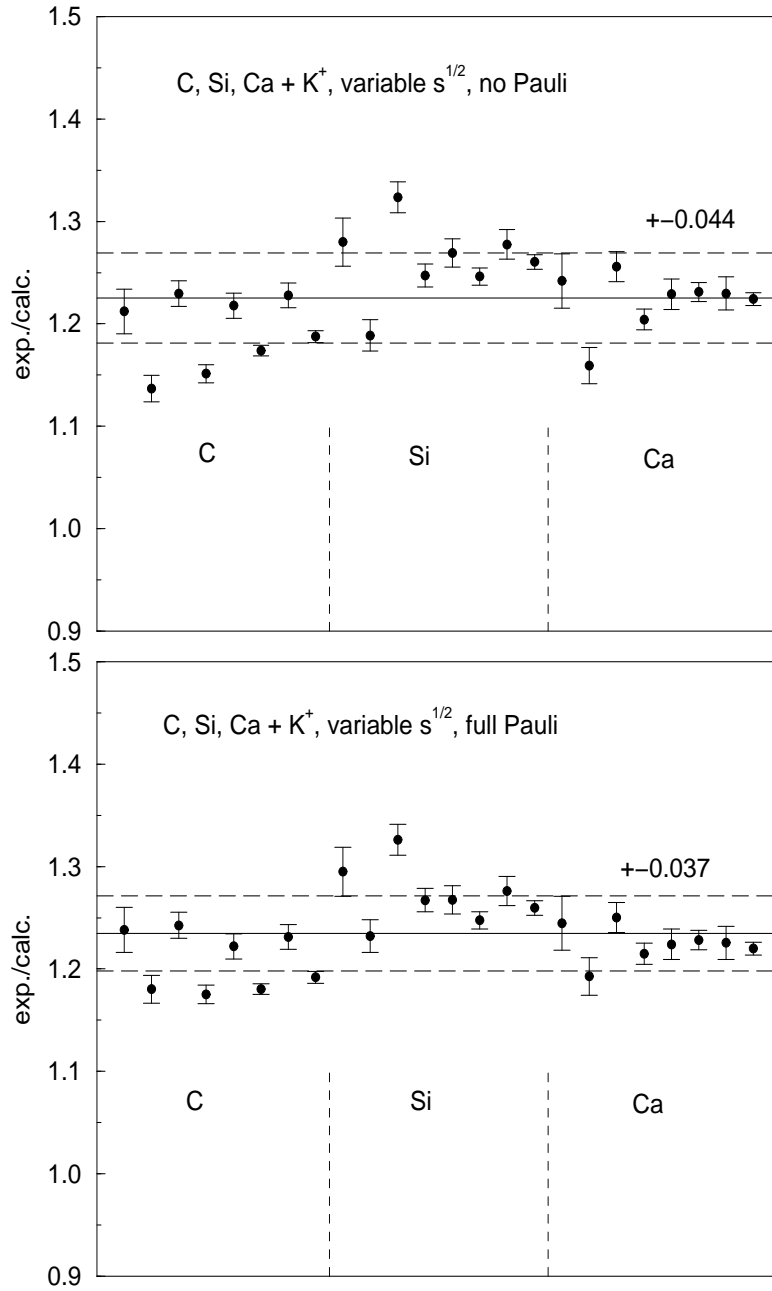


Figure 5: Experimental to calculated ratios of reaction and total cross sections on C, Si and Ca for variable energies Eq.(7) (top), and with Pauli correlations also included (bottom).

there is a systematic difference between calculated and experimental dependence on energy of the cross sections. The bottom part of Fig. 4 shows similar results for calculations based on the full variable energy of Eq.(7) and it is evident that the energy dependence is reproduced very well by calculations. The value of T_N (Eq.(7)) was adjusted to the low density of ${}^6\text{Li}$. Adding also the Pauli correlations made very small difference. It is therefore seen that (i) From the energy-dependence of the ratios the prescription of Eq.(7) is supported by experiment and (ii) Effects due to Pauli correlations are very small for the low-density ${}^6\text{Li}$ nucleus.

Turning to the other target nuclei, namely C, Si and Ca, calculations with fixed energies (not shown) display systematic deficiencies regarding the variation with energy of the experimental to calculated ratios, similarly to the results for ${}^6\text{Li}$. Figure 5 (top) shows the ratios obtained using the \sqrt{s} algorithm Eq.(7) but without the Pauli correlations corrections of WRW. The energy dependence of the ratios for the reaction cross sections is seen to be well reproduced by the calculations but there is a residual disagreement in the energy dependence for the total cross sections, notably for C. The bottom part of Fig. 5 shows these ratios where the WRW in-medium corrections have also been included, and the improved agreement is evident. The larger scatter of the ratios for Si has been observed also in earlier analyses [29].

3.2. In-medium enhancement

Agreement to 2-3% between calculation and experiment for the reaction and total cross sections on the very low density ${}^6\text{Li}$, as obtained above, had not been observed in earlier analyses. Consequently we deal here directly with the cross sections for the ‘normal’ targets of C, Si and Ca, without the use of ‘super-ratios’, namely, without normalizing experimental to calculated ratios for a given target to the corresponding ratios for ${}^6\text{Li}$. Moreover, with the present model for variations of the in-medium energies we try to fit calculations to experiment for the three targets at the four energies put together, a total of 24 data points.

The first phenomenological approach is to simply multiply separately the real and the imaginary parts of the amplitudes by a respective scaling factor, the same for all energies and four targets. Obviously no fit to the data is possible with ${}^6\text{Li}$ included because for ${}^6\text{Li}$ no scaling factors are expected whereas this is not the case for C, Si and Ca. Removing ${}^6\text{Li}$ from the data, fits of two parameters to the three heavier targets yields for 24 data points $\chi^2=23.8$ when using assigned errors of $\pm 3.7\%$ as implied by the scatter of the

ratios of calculated to experimental cross sections (see Fig. 5). The scaling factors are then $F_R=0.87\pm 0.10$ for the real part and $F_I=1.41\pm 0.02$ for the imaginary part of the potential. A separate fit to the eight ${}^6\text{Li}$ cross sections leads to $\chi^2=8.7$ with scaling factors of 0.71 ± 0.10 and 1.02 ± 0.02 for the real and imaginary parts, respectively. Reducing the assigned errors all the way down to the statistical errors does not change the resulting scaling factors. Consequently we conclude that the real part of the amplitudes needs rescaling by 0.9 ± 0.1 whereas the imaginary part needs rescaling by 1.40 ± 0.02 in order to fit the reaction and total cross sections on C, Si and Ca.

Alternatives to rescaling of the input amplitudes have been tried too by adding a phenomenological term to the potential in order to fit the C, Si and Ca cross sections. Fits were possible by adding a term with higher powers of density than linear, to simulate two-nucleon processes. Another version was to add a linear term as a P -wave potential of the Kisslinger type [1]. Both options could close the 23% gap between the calculated cross sections based on the input amplitudes and experiment. However, comparisons with the few available results on the elastic scattering of K^+ by C did not support such approaches.

Out of the few experiments below 800 MeV/c we chose elastic scattering of K^+ by C at 715 MeV/c [34]. In Fig. 6 the dashed curve shows the predictions made using the present model with in-medium kinematics and WRW Pauli correlations effects. The solid curve shows the results when the above rescaling factors F_R and F_I are applied to the real and imaginary parts, respectively, to fit the (enhanced) reaction and total cross sections. Both are in fair agreement with experiment, showing very little sensitivity of the angular distribution to modifications required to fit the reaction and total cross sections. The option of adding a phenomenological non-linear term or a linear P -wave term to the potential (not shown), produced angular distributions that disagree sharply with experiment beyond the first minimum. Another attempt was to use for the in-medium forward scattering amplitudes only the S -wave amplitudes from SAID [21], thus neglecting the contributions from the P - and D -wave terms, and to add an explicit phenomenological P -wave potential [1]. That too made it possible to fit the reaction and total cross section with only two parameters. In this case the balance between repulsive and attractive real parts of the potential changed and the predicted angular distribution, dot-dashed curve in Fig. 6, is acceptable. Very similar results were obtained with K^+ elastically scattered by C at 635 MeV/c [34].

We have also checked if it was possible to include ${}^6\text{Li}$ in the data and to

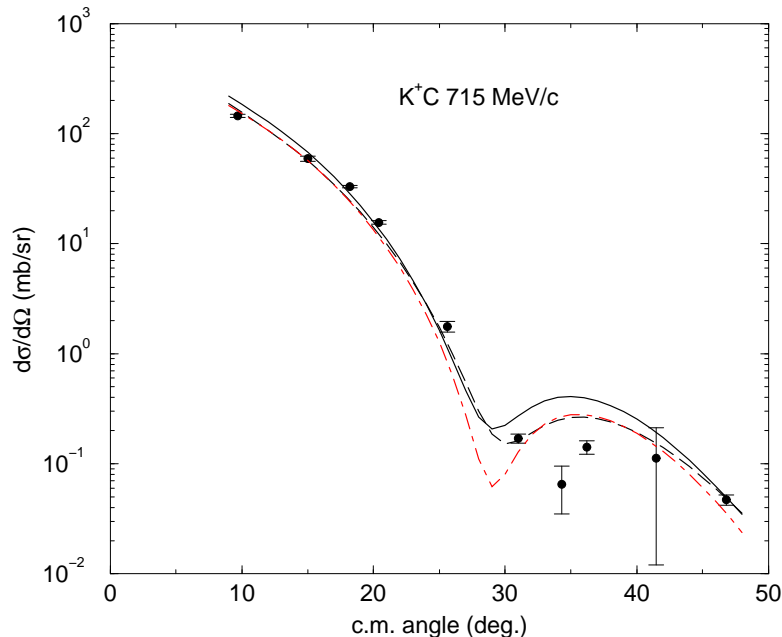


Figure 6: Calculated and experimental differential cross sections for elastic scattering of 715 MeV/c K^+ by C. Experimental results are from Ref. [34]. Dashed curve for amplitudes without rescaling, solid curve for rescaling by constants, dot-dashed curve for added phenomenological p -wave potential, see text.

fit all 32 cross sections with additional terms in the potential. This approach failed before [28, 29] and it has likewise failed in the present work. However, it was shown in Ref. [28, 29] that a possible way to handle ${}^6\text{Li}$ and the other targets together was by using as a parameter an *average* density of the nucleus that turns out to cut-off ${}^6\text{Li}$ from the rescaling of the imaginary potential. In this model the real part of the potential is rescaled by a constant whereas the imaginary part is multiplied by the expression

$$F_1 = [1 + \text{Im}B_0(\bar{\rho} - \rho_c)\Theta(\bar{\rho} - \rho_c)] \quad (10)$$

with $\bar{\rho}$ the average density of the target nucleus and ρ_c a cut-off density. With ρ_c turning out to be $0.088 \pm 0.005 \text{ fm}^{-3}$, larger than the average density of the ${}^6\text{Li}$ nucleus, it was possible to fit all 32 data points with only three parameters. The predicted angular distribution for elastic scattering of 715 MeV/c K^+ by C when using this prescription is indistinguishable from the solid curve in Fig. 6.

4. Discussion and summary

Recent in-medium algorithm for calculating optical potentials from the respective meson-nucleon forward scattering amplitudes, used so far for kaonic atoms, pionic atoms, low energy pion scattering and η -nucleus interactions, was used in the present work to calculate integral cross sections for low energy K^+ mesons. This work was motivated by better penetrability of kaons into nuclei below 800 MeV/c in comparison with other particles thus providing more sensitive tests of this approach. In particular, penetration beyond the nuclear surface into where the density is close to the full nuclear density means shifts of up to 30 MeV in the argument of the in-medium amplitude which causes observable effects. It was possible to test separately the effects of the energy-dependence implied by the model and the importance of applying corrections due to Pauli correlations. Both were found to improve the agreement between experiment and calculations regarding the energy-dependence of total and reaction cross sections of K^+ on C, Si and Ca, particularly at the lower energy end of the range.

For the low-density ${}^6\text{Li}$ nucleus, calculation and experiment agree to better than 3% uniformly over the energy range studied when the variable energy of the model is applied. Effects due to Pauli correlations are negligibly small. Compared with earlier analysis [27, 28, 29] the full agreement achieved for ${}^6\text{Li}$ is partly due to the inclusion in the present work of D -wave contributions to the forward scattering amplitude. The D_{03} partial wave contributes attraction that is close to 30% of the repulsion due to the S_{11} partial wave, particularly at the lower energies.

The ${}^6\text{Li}$ provides a solid basis for direct comparisons with the other three nuclear targets without a need to use so-called ‘super-ratios’, namely, normalizing experimental to calculated ratios for a target to the corresponding ratios for ${}^6\text{Li}$. The experimental cross sections for C, Si and Ca are found to be $(23\pm 4)\%$ larger than calculation, in general agreement with previous observations. This enhancement could be reproduced phenomenologically by rescaling the imaginary part of the potential by $40\pm 2\%$ but quantitative understanding of this effect could not be achieved. It suggests that in-medium enhancements of K^+ -nucleon interaction are due to more exotic mechanisms than traditional corrections. Comparisons with predictions of such mechanisms are obviously called for.

Acknowledgements

Fruitfull discussions with A. Gal are gratefully acknowledged.

References

- [1] L.S. Kisslinger, Phys. Rev. 98 (1955) 761
- [2] M. Ericson, T.E.O. Ericson, Ann. Phys. 36 (1966) 323.
- [3] E. Friedman, Phys. Rev. C 28 (1983) 1264.
- [4] G.R. Satchler, Nucl. Phys. A 540 (1992) 533.
- [5] M.B. Johnson, G.R. Satchler, Ann. Phys. 248 (1996) 134.
- [6] D.V. Bugg et al., Phys. Rev. 168 (1968) 1466.
- [7] Y. Mardor et al., Phys. Rev. Lett. 65 (1990) 2110.
- [8] R.A. Krauss et al., Phys. Rev. C 46 (1992) 655.
- [9] R. Sawafta et al., Phys. Lett. B 307 (1993) 293.
- [10] R. Weiss et al., Phys. Rev. C 49 (1994) 2569
- [11] A. Cieplý, E. Friedman, A. Gal, D. Gazda, J. Mareš, Phys. Lett. B 702 (2011) 402.
- [12] A. Cieplý, E. Friedman, A. Gal, D. Gazda, J. Mareš, Phys. Rev. C 84 (2011) 045206.
- [13] E. Friedman, A. Gal, Nucl. Phys. A 881 (2012) 150.
- [14] D. Gazda, J. Mareš, Nucl. Phys. A 881 (2012) 159.
- [15] E. Friedman, A. Gal, Nucl. Phys. A 899 (2013) 60.
- [16] E. Friedman, A. Gal, J. Mareš, Phys. Lett. B 725 (2013) 334.
- [17] A. Cieplý, E. Friedman, A. Gal, J. Mareš, Nucl. Phys. A 925 (2014) 126.
- [18] E. Friedman, A. Gal, Nucl. Phys. A 928 (2014) 128.

- [19] E. Friedman, A. Gal, B. Loiseau, S. Wycech, Nucl. Phys. A 943 (2015) 101.
- [20] E. Friedman, A. Gal, Phys. Rep. 452 (2007) 89.
- [21] <http://gwdac.phys.gwu.edu>
- [22] P.B. Siegel, W.B. Kaufmann, W.R. Gibbs, Phys. Rev. C 31 (1985) 2184.
- [23] G.E. Brown, C.B. Dover, P.B. Siegel, W. Weise, Phys. Rev. Lett. 60 (1988) 2723.
- [24] M.F. Jiang, D.S. Koltun, Phys. Rev. C 46 (1992) 2462.
- [25] C. Garcia-Recio, J. Nieves, E. Oset, Phys. Rev. C 51 (1995) 237.
- [26] J.C. Caillon, J. Labarsouque, Phys. Rev. C 53 (1996) 1993.
- [27] E. Friedman et al., Phys. Rev. C 55 (1997) 1304.
- [28] E. Friedman, A. Gal, J. Mareš, Phys. Lett. B. 396 (1997) 21.
- [29] E. Friedman, A. Gal, J. Mareš, Nucl. Phys. A 625 (1997) 272.
- [30] R.J. Peterson, Phys. Rev. C 60 (1999) 022201.
- [31] A. Gal, E. Friedman, Phys. Rev. Lett. 94 (2005) 072301.
- [32] A. Gal, E. Friedman, Phys. Rev. C 73 (2006) 015208.
- [33] T. Waas, M. Rho, W. Weise, Nucl. Phys. A 617 (1997) 449.
- [34] R.E. Chrien, R. Sawafta, R.J. Peterson, R.A. Michael, E.V. Hungerford, Nucl. Phys. A 625 (1997) 251.